JOURNAL OF GEOPHYSICAL RESEARCH, VOL. 94, NO. D14, PAGES 16,797–16,813, NOVEMBER 30, 1989

Evidence for Diabatic Cooling and Poleward Transport Within and Around the 1987 Antarctic Ozone Hole

M. H. PROFFITT,[1] K. K. KELLY, AND J. A. POWELL[1]

NOAA Aeronomy Laboratory, Boulder, Colorado

B. L. GARY

Jet Propulsion Laboratory, Pasadena, California

M. LOEWENSTEIN, J. R. PODOLSKE, S. E. STRAHAN, AND K. R. CHAN

NASA Ames Research Center, Moffett Field, California

Combining in situ measurements of nitrous oxide, total water, and NO_y with meteorological data, including potential vorticity, taken during the 1987 Airborne Antarctic Ozone Experiment, a consistent picture emerges of a gradual poleward movement of air extending from about 10° in latitude outside the boundary of the ozone hole to about 5° inside. The data analysis is concentrated in the potential temperature range of 425–450 K, corresponding to geometric altitudes of 17.5–19 km. Evidence of ongoing diabatic cooling throughout this region is presented, and cooling rates of about 1.75 K in potential temperature per day (approximately 0.8 K per day in temperature at constant pressure) are calculated from the data outside the boundary of the ozone hole. An interpretation of the data is presented that describes the movement of air that has come from lower latitudes into the ozone hole, as diabatically descending and spiraling poleward. The result of this spiraling motion is a dominantly advective flow of ozone rich air across the boundary and into the ozone hole. This simple picture precludes requiring extensive isentropic mixing with accompanying vertical descent to maintain the steep poleward isentropic gradients found in nitrous oxide. Data are presented to show that the necessary accompanying outflow of stratospheric air from within the ozone hole occurs at potential temperatures less than 425 K and that, during the mission, there was no significant transport of processed air across the boundary and out of the ozone hole from 425 to 450 K. Arguments involving conservation of angular momentum are also used to support this model.

INTRODUCTION

The 1987 Airborne Antarctic Ozone Experiment (AAOE) was conducted out of Punta Arenas, Chile, from mid-August until late September. There were two aircraft involved in the mission, an ER-2 covering altitudes up to about 19 km and a DC-8 that was limited in altitude to about 13 km. Details of the instrumentation and general flight logistics have been given elsewhere [*Tuck et al.*, 1989].

In considering the global impact of the ozone hole, a prime issue is whether there is poleward flow of lower latitude ozone-rich stratospheric air into the region of large ozone loss, with a concurrent equatorward flow of processed ozone-poor air returning to lower latitudes possibly at a different altitude. If there were such a flow, the ozone hole would act as a flowing processor of ozone and would not only be a source of air depleted of ozone, but also a source of denitrified [*Fahey et al.*, 1989, this issue] and dehumidified [*Kelly et al.*, 1989] air that is carrying an abundance of reactive chlorine that could, for a time, continue to destroy ozone. In contrast, if the air within the region of large ozone loss were locked in place during the evolution of the ozone hole, its effect could be considerably less. Therefore, knowing the poleward flow rates, if any, the altitude range of the flow, and its return path to lower latitudes is crucial in evaluating the mass of ozone destroyed and the significance of the effect of the ozone hole at other latitudes. These are the issues we will consider in this paper.

The region of high ozone loss associated with the Antarctic ozone hole is collocated with the region of high ClO values [*Anderson et al.*, 1989*a*; *Proffitt et al.*, this issue] and is referred to as the chemically perturbed region. The boundary of the chemically perturbed region has been defined at potential temperatures of 425 and 450 K by a level of ClO (130 ppbv) and found to be coincident with dramatic poleward isentropic decreases in ozone, NO_y, and NO. Decreases in H_2O, N_2O, potential vorticity (here a negative quantity, so increasing in absolute value), temperature, and wind speed are also observed but are not generally as dramatic [*Proffitt et al.*, 1989]. The decreases in ozone, NO_y, N_2O, and H_2O imply there is little bidirectional horizontal flow across the boundary (therefore some authors have adopted the notion of a "chemical containment vessel"). The potential vorticity and wind speed decreases imply that this sharp boundary, that is defined chemically, is maintained dynamically. The usefulness of this boundary for identifying a reference latitude for comparison of ER-2 data on a flight-by-flight basis has been demonstrated elsewhere [*Proffitt et al.*, 1989, this issue; *Fahey et al.*, this issue; *Hartmann et al.*, 1989, this issue], and we will continue

[1]Also at Cooperative Institute for Research in Environmental Science, University of Colorado, Boulder.

Paper number 89JD00799.
0148-0227/89/89JD-00799$05.00

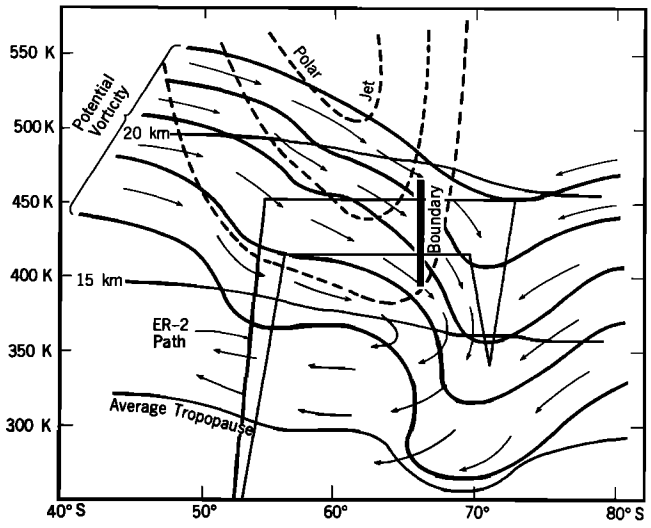

Fig. 1. Latitudinal cross section through the polar jet on a vertical grid of potential temperature. Position of polar jet (isotachs), potential vorticity isopleths, the boundary of the chemically perturbed region, the average tropopause height, and the approximate altitudes are indicated. A typical flight path for the ER-2 is also indicated. The arrows indicate the direction of flow of air parcels, following potential vorticity isopleths above 400 K, then, by mixing with air of lower potential vorticity, crossing those isopleths below 400 K.

those analyses here using temporal trends and temporal averages to address questions of dynamics.

In the following sections, nitrous oxide (a long-lived tracer), total water (water vapor with particulate water), NO_y (total odd nitrogen species), and potential vorticity (a dynamical tracer derived from pressures, temperatures, and wind speeds) are used to analyze atmospheric dynamics at our flight levels. The data used have come primarily from measurements made aboard the ER-2 high-altitude aircraft during the 1-month period of August 23 through September 22. Since most of the flight data were taken during the constant potential temperature flight legs at 425 ± 10 K and 450 ± 10 K, we have concentrated our analysis at those two levels, although some data are used from lower levels during ascents and descents near Punta Arenas and during altitude profiles within the ozone hole. We will interrelate many diverse measurements which may appear to be overly complicated, but what we hope to convey to the reader is the consistency of our dynamical model with this complete data set, whether examined as averages or as temporal trends. We now introduce the major parts of this paper and our Figure 1, which we hope will aid in following the arguments presented in the body of the paper.

In the next section of this paper, we use nitrous oxide (N_2O) data to show there was diabatic cooling (net heating or cooling reflected by a change in the potential temperature of an air parcel) in progress during the mission. We first present analyses of N_2O and ozone temporal trends at fixed latitudes as an introduction to the data and to emphasize the importance of calculating trends relative to the boundary of the chemically perturbed region. Using the boundary as a reference point, we then present detailed analyses of N_2O to show there was ongoing diabatic cooling at our flight altitudes on both sides of the boundary. Potential vorticity calculations are then used to show that the cooling was spatially uniform and that the descending motion, due to diabatic cooling, produced a poleward flow across the boundary. We then elaborate on the poleward transport and show by using N_2O, NO_y, and total water data that there is little outward mixing across the boundary at 425–450 K and that a northward outflow seems to occur below 400 K. By combining the results of these sections, it is next shown that the flow is dominantly advective. In the last two sections, total water temporal trends are used to obtain a diabatic cooling rate outside the boundary, and a brief analysis of the angular momentum budget is given.

From these diverse measurements emerges a consistent picture of air slowly advecting from lower latitudes and diabatically descending with a strong poleward component that carries stratospheric air, rich in ozone, into the ozone hole. Although we have concentrated our analysis at 425 and 450 K, a larger picture of the general circulation in the lower stratosphere near the polar jet can be inferred in a format that may prove helpful for the reader to reference when following the arguments presented in this paper. Therefore we present Figure 1 as a qualitative representation of some aspects of the dynamics of the vortex. The figure depicts contours of constant zonal wind speed (isotachs) on a coordinate system of latitude versus potential temperature. Altitudes and an approximate tropopause are given for reference along with a typical flight track for the ER-2. Over this complex grid, we superimpose potential vorticity isopleths and arrows to indicate the direction of movement of air parcels in the plane of the figure. Other features of Figure 1 will be discussed later. Clearly this cross section does not represent the zonal motion of an air parcel being carried around the pole by the jet, with its characteristic circuit time of about 1 week. We must picture the poleward progression of an air parcel as a spiraling and descending motion, but our figure excludes the important zonal component. Our cross section qualitatively incorporates data taken on ER-2 ascents, descents, and high-latitude altitude profiles as well as features found in standard meteorological data taken during the mission [*Newman et al.*, 1988]. One should bear in mind that the ER-2 data are restricted to a somewhat limited latitude range (53°S–72°S) and to a very limited longitude range (about 65°W) near the Antarctic Peninsula and that our conclusions may not apply around the entire vortex. Furthermore, these conclusions are made by primarily considering spatially and temporally averaged data along with temporal trends and are considered to be representative of the overall average during the mission rather than representing daily processes. For a flight-by-flight analysis of the data, the reader is referred to papers in AAOE volume 1 [*Tuck*, 1989; *Kelly et al.*, 1989].

DIABATIC COOLING

Evidence of ongoing diabatic cooling from whole-air samples and correlations between trace species has been shown elsewhere [*Tuck*, 1989; *Murphy et al.*, 1989; *Toon et al.*, this issue]. Tuck argues, by using the $CFCl_3/N_2O$ ratio, that cooling rates as high as 4–6 K in potential temperature per day were present within the boundary during certain periods. Toon uses column HF measurements to show there was an average descent rate of about 85 m/d, but by examining temporal trends in $CFCl_3$, CF_2Cl_2, N_2O, and CH_4, no descent was evident. In the next section we will use N_2O

spatial distributions and temporal trends to conclude that there was ongoing diabatic cooling both within the chemically perturbed region and for a few degrees in latitude outside the chemically perturbed region.

Nitrous Oxide

The suitability of N_2O as a tracer stems from it being photochemically almost inert at these altitudes. The photochemical lifetime of N_2O decreases with increasing altitude, starting at about 100 years at altitudes up to 22 km, 10 years at 28 km, 1 year at 33 km, and less than 1 month above about 40 km [*Brasseur and Solomon*, 1986]. Therefore we can depend on the N_2O content of any particular air parcel to remain constant at our flight levels over the duration of the mission. Since its source is at the ground and its stratospheric sink increases dramatically with altitude and decreases with latitude, vertical profiles of N_2O can be used as indicators of the general circulation scheme of the atmosphere.

The N_2O measurements used in this section are entirely from the ER-2 ATLAS instrument [*Podolske et al.*, this issue], an instrument with a 1-s measurement time, rather than the whole-air sampler [*Heidt et al.*, 1989] that sampled a maximum of 14 times on a flight. An intercomparison of the N_2O measurements made simultaneously by these two instruments along the flight path showed good agreement except for an offset between them of about 30 ppbv, with the ATLAS measurements being the lower. This difference has not been fully resolved and will be referred to later in this paper.

We now consider temporal trends in N_2O that have been determined by different methods and show evidence of diabatic cooling over the flight period of August 23 through September 22. Our first method is to analyze the temporal trends at two fixed latitudes, one outside the ozone hole at 53°S on ascent out of Punta Arenas, the other at our maximum latitude within the ozone hole at 72°S. Then we will consider the data referenced to the boundary but at many positions both inside and outside the boundary.

Temporal Trends at 53°S and 72°S

At both 53°S and 72°S the N_2O measurements at potential temperatures of 400 and 425 K show no systematic trend over the 1-month period but do show large variations (see Figure 2). Within these large variations there is a clear signature at both latitudes of relatively small values from August 30 through September 9 when compared with flights before or after those dates. A similar signature can be seen in the ozone temporal trends given in Figures 3*a* and 3*b*, but with relatively large values during this same period. Therefore both the N_2O and ozone data indicate that air sampled during this period is of higher stratospheric origin (although at the same potential temperature) and not the same air sampled on the other flights. Clearly, temporal trends derived in this fashion are of questionable value. Since N_2O is a more conservative tracer than potential temperature, ozone temporal trends calculated at constant values of N_2O should be more representative for trend analysis of a fixed air parcel. *Anderson et al* [1989*b*] have used such analyses elsewhere. By comparing ozone temporal trends at a constant potential temperature (Figures 3*a* and 3*b*) with those for constant N_2O (Figures 3*c* and 3*d*), we see that the scatter

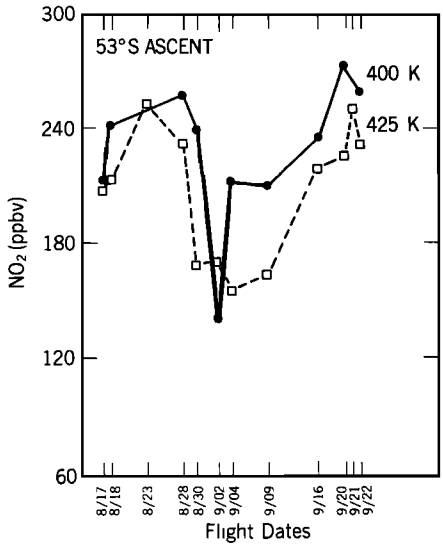

Fig. 2*a*

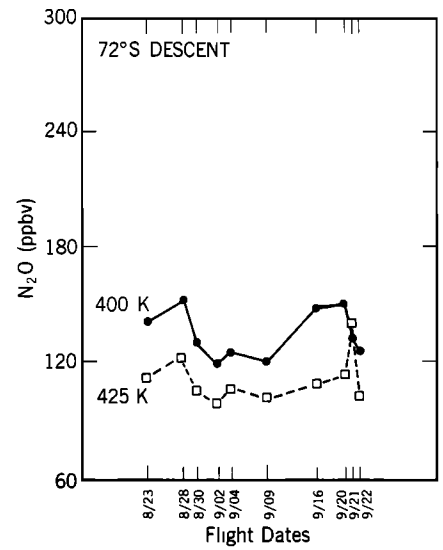

Fig. 2*b*

Fig. 2. N_2O temporal trends during mission for potential temperatures of 400 and 425 K at (*a*) 53°S latitude on ascent out of Punta Arenas, Chile, and (*b*) 72°S latitude on descent within the ozone hole.

is reduced in the latter. Fortuitously, the slopes of the linear fits to the data in Figure 3*b* are almost identical to those of Figure 3*d*. By referencing data to constant N_2O during ascents and descents, we may reduce the scatter in the temporal trends of ozone, but given that the data set is primarily from isentropic flight legs (long portions of the flights at constant potential temperatures), this is not the best way to determine whether the potential temperature of a fixed parcel is changing (that is, undergoing net heating or cooling). This we will accomplish by considering isentropic temporal trends (trends at a constant potential temperature) of our long-lived conservative tracer, N_2O, but now with a horizontal reference other than latitude. As we discussed in the introduction, degrees latitude from the boundary of the chemically perturbed region serves as a suitable replacement for latitude alone.

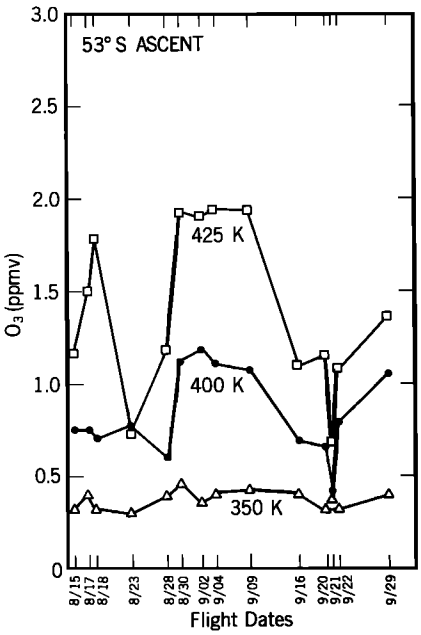

Fig. 3a

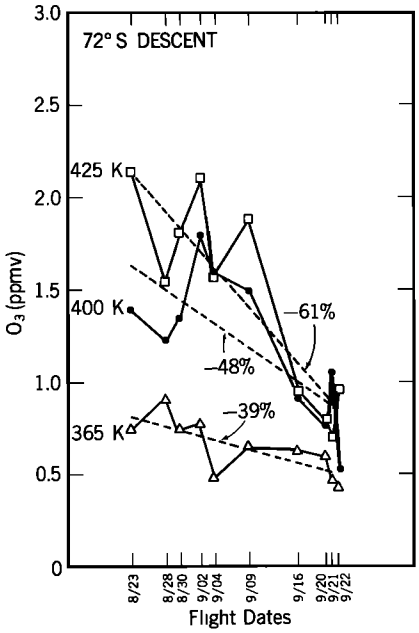

Fig. 3b

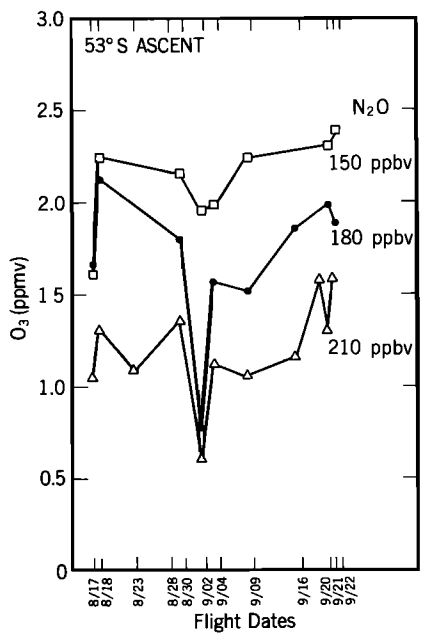

Fig. 3c

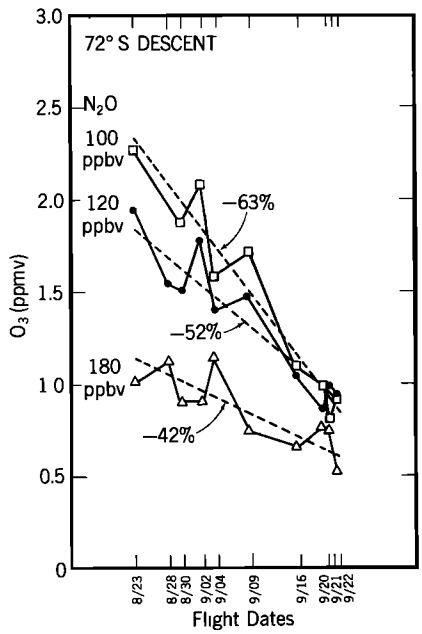

Fig. 3d

Fig. 3. Ozone temporal trends during mission on ascent at 53°S latitude and at 72°S latitude. (*a*, *b*) Determined as for N_2O in Figure 2. (*c*, *d*) Trends are determined for constant values of N_2O rather than constant potential temperature. (*b*, *d*) Linear least squares fits to the data and percent decreases over the 1-month period of August 23 through September 22 are included.

Temporal Trends With Respect to the Boundary

We will introduce the data referenced to the boundary by first considering Figure 4, which shows N_2O versus latitude relative to the boundary for the two potential temperature flight levels of 425 and 450 K. The plots were obtained by averaging the flight leg data in 1° latitude bins relative to the boundary and by including in that average all data with an average potential temperature within 10 K of either 425 or 450 K. Averages include all of the 10 ER-2 flights that penetrated the boundary. The error bars indicate the scatter in the data and are calculated as the sample standard deviation of the N measurements comprising the average, with N given directly below the error bar. To obtain the standard deviation of the mean, simply divide our result by the square root of $N - 1$. It should first be noted that the number of measurements at the 450 K level is much less than at the 425 K level for comparable positions relative to the

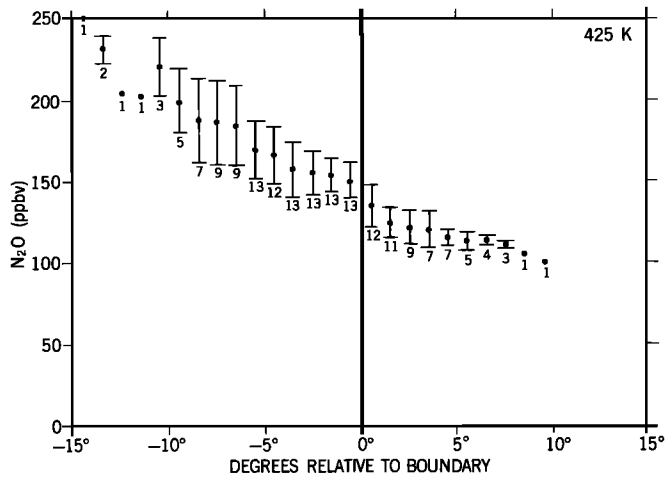

Fig. 4*a*

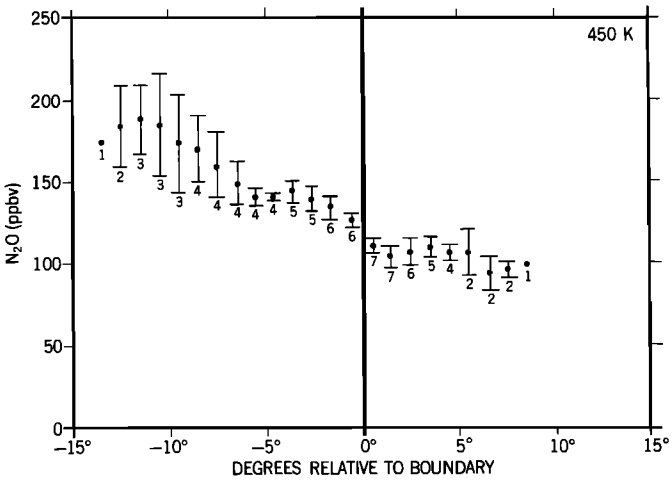

Fig. 4*b*

Fig. 4. Plots of averaged N_2O versus latitude referenced to the boundary of the chemically perturbed region (heavy vertical line) for the (*a*) 425 K and (*b*) 450 K flight levels. Data are averaged over 1° latitude intervals and over all flight data from August 23 through September 22.

boundary. This means that fewer flight legs were flown at the upper level and that the statistics are not as reliable. In both plots we can see a clear decrease in N_2O with increasing latitude, and a clear decrease with altitude for comparable positions relative to the boundary. From this we can see that calculating temporal trends in ozone for constant N_2O values, without regard for the position of the data with respect to the boundary as we did in the previous section, will also be less than ideal, as the potential temperature will not be held constant. A better method would be to determine trends for constant values of N_2O and constant position relative to the boundary. Unfortunately, there are insufficient data for this method, but since flight legs were usually flown at constant potential temperatures, we will instead return to potential temperature and calculate trends in N_2O at constant potential temperatures and fixed positions relative to the boundary. In this way, we will gain insight into the diabatic processes at flight levels by looking for temporal changes over this 1-month period to indicate air of different origin, but at fixed positions with respect to the boundary. We present these detailed arguments to impress upon the reader the importance of calculating temporal averages and temporal trends relative to this frame of reference in place of latitude.

The 1-month ozone trends from August 23 through September 22 were calculated at various positions relative to the boundary, and they revealed that this boundary accurately locates the region of large temporal ozone decrease [*Proffitt et al.*, 1989, this issue]. Figures 5 and 6 show N_2O data at different positions relative to the boundary on the various flights. Temporal trends in the data within the boundary at 425 K are also indicated as linear least squares fits to that data. Table 1 summarizes the results of calculating temporal trends for each panel in Figure 5 and Figure 6. Also included in Table 1 are potential vorticity, total water, and alternate N_2O trend calculations (all to be discussed later), the average potential temperatures measured concurrent with the N_2O measurements represented in Figures 5 and 6, and the temporal trends in potential temperature along the flight legs to indicate the consistency of the constant potential temperature flight legs. In all cases, the numbers indicated as the error range are the standard deviations of the residuals expressed in percent of the midpoint value derived from the linear fit. The numbers given in parentheses are the number of data points (flight legs) used to determine the temporal trends on that line.

Table 1 and Figure 6 are now evaluated from two viewpoints: (1) are there enough data points throughout the time period to justify a trend analysis?, and (2) which trends are significantly different from zero? Addressing the first question, by considering the data in Figure 6, it appears that all latitudes except those outside the boundary at 450 K have data covering more than 3 weeks of the 1-month period, and that is considered here to be adequate. The need for obtaining trends outside the boundary at 450 K will be addressed in the alternate method for computing N_2O trends. The second question can be answered by considering the figures for qualitative evaluation and by considering the standard deviation of the residuals given in Table 1 for quantitative evaluation. Each residual indicates how closely the data points fit the straight line determined by the linear least squares fit. For those cases where the residual is comparable to or greater than the calculated trend, the trend is not considered significant, and the uncertainty is approximated by the residual. Considering these comments, we conclude that at 425 K, there are significant downward trends, averaging 18% over the 5° inside the boundary, but practically no significant trends outside. At 450 K, there are relatively small downward trends inside the boundary, but due to lack of data outside, little can be concluded.

In order to obtain temporal trends outside the boundary at 450 K that would be meaningful, and to check the method just described to see if trends in potential temperature due to systematic changes in flight levels could be influencing the N_2O trends, a second method was also used. The flight on August 23 was not flown on constant potential temperature surfaces as were the other flights, but attained potential temperatures outside the boundary that were well above the range considered for the trend calculations from the 450 K legs (above 460 K). Since N_2O has a fairly well-defined potential temperature dependence from 425 K up to 450 K as determined from the many flights made during this 1-month period, the data points from August 23 that are outside the boundary and above the 460 K limit have been referenced to

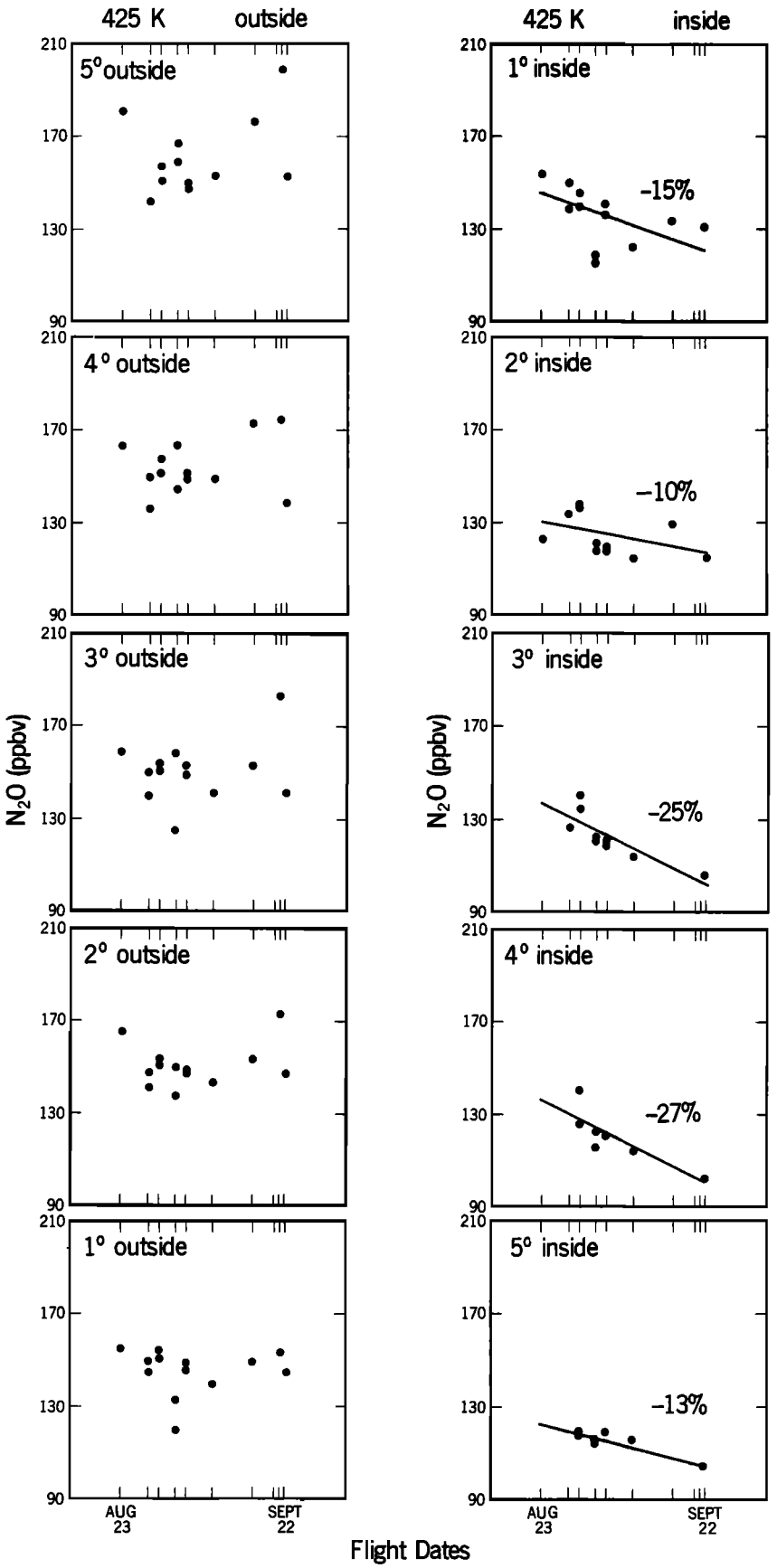

Fig. 5. N_2O temporal trends at 425 K relative to the boundary of the chemically perturbed region. Plots form series starting from upper left corner at 5° latitude north of the boundary to lower left corner, then beginning at upper right and ending at lower right corner at 5° latitude south of the boundary. Straight lines indicated for data inside boundary are linear least squares fits to the data.

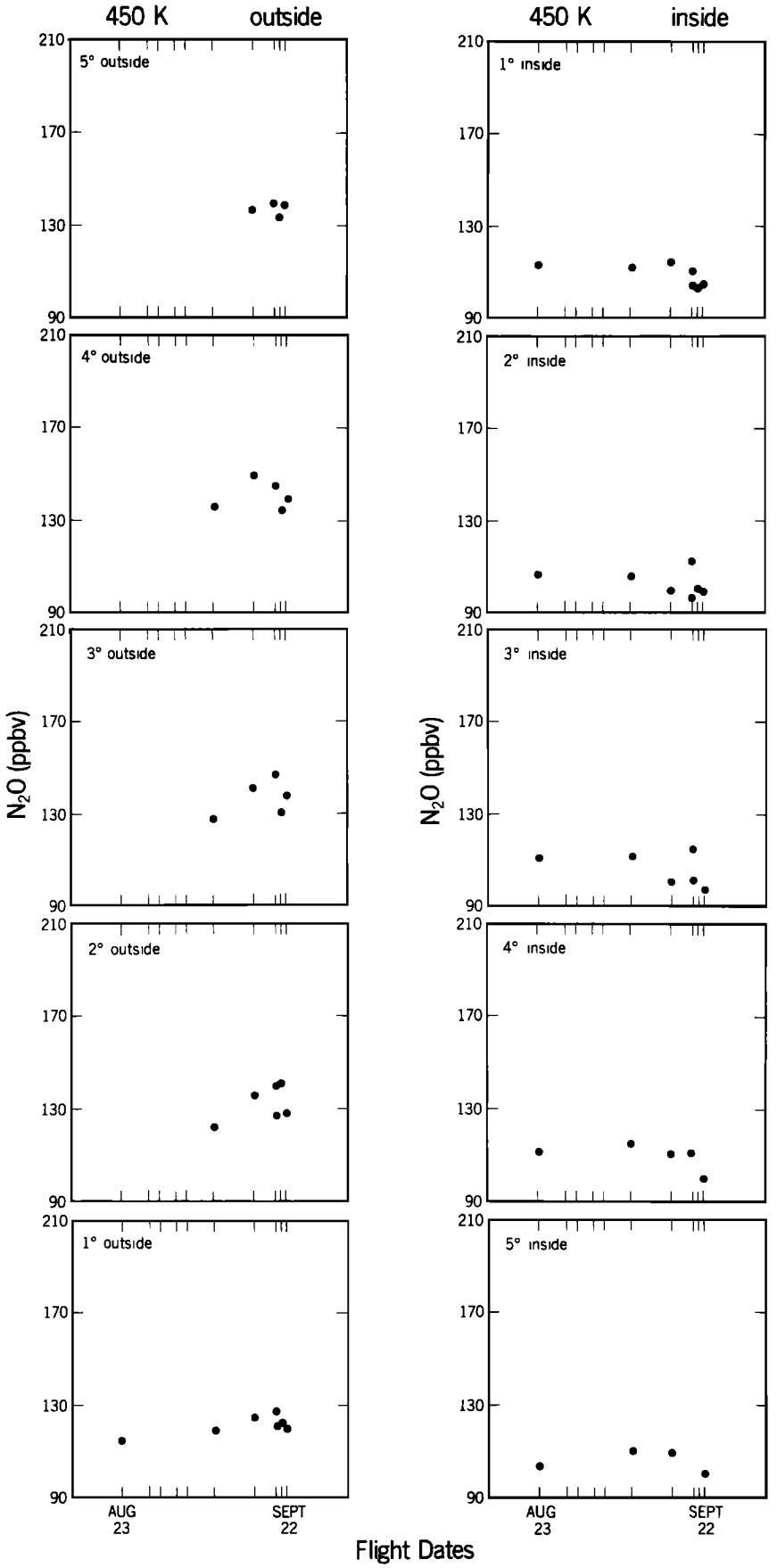

Fig. 6. N_2O temporal trends as in Figure 5 except at 450 K.

TABLE 1. One-Month Temporal Trends

Degrees Relative to Boundary	N_2O, %	ALT N_2O, %	Potential Vorticity, %	H_2O, %	Temperature	
					Potential, %	Average, K
			425 ± 10 K (Outside)			
−5 (13)	+12 ± 10	+17 ± 10	−14 ± 7	+19 ± 3	+1.5 ± 1.0	423
−4 (13)	+6 ± 8	+9 ± 8	−5 ± 14	+14 ± 3	+0.9 ± 1.0	424
−3 (13)	+7 ± 9	+9 ± 8	−8 ± 6	+11 ± 3	+0.6 ± 0.9	423
−2 (13)	+4 ± 7	+7 ± 6	−15 ± 5	+18 ± 3	+1.1 ± 0.7	424
−1 (13)	0 ± 7	+5 ± 5	−26 ± 7	+18 ± 2	+1.6 ± 1.0	424
			425 ± 10 K (Inside)			
+1 (13)	−15 ± 5	−14 ± 7	−30 ± 9	+3 ± 6	+0.3 ± 1.2	425
+2 (11)	−10 ± 7	−12 ± 25	−27 ± 9	−13 ± 9	−1.1 ± 1.1	426
+3 (9)	−25 ± 6	−25 ± 8	−27 ± 8	−31 ± 9	+0.0 ± 1.3	426
+4 (7)	−27 ± 6	−25 ± 7	−26 ± 7	−42 ± 14	+0.7 ± 1.0	424
+5 (7)	−13 ± 2	−17 ± 1	−8 ± 8	−29 ± 15	−1.5 ± 0.3	422
			450 ± 10 K (Outside)			
−5 (5)		−18 ± 3				
−4 (6)		−1 ± 6				
−3 (6)		+3 ± 6				
−2 (7)		+4 ± 4				
−1 (7)	+9 ± 3	+1 ± 5		+16 ± 6	+1.5 ± 1.0	453
			450 ± 10 K (Inside)			
+1 (7)	−6 ± 9	−5 ± 3		0 ± 6	+0.3 ± 0.8	451
+2 (7)	−7 ± 6	+3 ± 4		+11 ± 8	+2.7 ± 0.9	450
+3 (6)	−7 ± 7	+1 ± 5		+12 ± 9	+2.7 ± 0.7	448
+4 (5)	−6 ± 5	−1 ± 4		−14 ± 15	+1.4 ± 0.7	446
+5 (4)	−2 ± 5	+8 ± 3		+24 ± 14	+2.8 ± 1.0	444

Temporal trends from August 23 through September 22, 1987. Temporal trends indicate linear fit to temporal data during 1-month period, and error limits are the residuals of linear fit. The numbers in parentheses are the number of data points used in the trend analysis. The average potential temperature is also given.

450 K for an alternate analysis. In addition, as a consistency check, the N_2O trends we previously described were reanalyzed with this alternate analysis. This was achieved in the following manner. N_2O isopleths on a latitude versus potential temperature grid are given elsewhere in this issue [*Podolske et al.*, this issue]. From their plot we calculated the slopes of N_2O versus potential temperature at fixed latitudes between 425 and 450 K. Average values of −1.07 ppbv per degree potential temperature outside the boundary and −0.8 ppbv per degree potential temperature inside the boundary were calculated. Then each point used in the alternate trend analysis, (N_2O alt) was calculated by adding to each measured N_2O data point in Figures 5 and 6 (N_2O meas) the product of the appropriate constant (inside or outside), Γ, with the deviation of the potential temperature for that data point, Θ meas, from the reference temperature, Θ ref, (425 or 450 K). That is,

$$(N_2O \text{ alt}) = (N_2O \text{ meas}) + \Gamma \times (\Theta \text{ meas} - \Theta \text{ ref})$$

The results of the trend calculations are given in Table 1 and, except at 450 K outside the boundary, are very consistent with those trends without the normalization. Outside the boundary at 425 K, there appears to be a slight positive trend, but the values are near the residual values except in the latitude bin farthest from the boundary. Being the farthest from the reference latitude of the boundary, it is the least reliable. Therefore no significance will be attached to the trends outside the boundary at 425 K, although there is a positive trend averaging 9% indicated in this region by one method and 6% in the other, but with large residuals. The region inside the boundary at 425 K has remained essentially unchanged from the first analysis, now with an average decrease of 19%. The 450 K level has changed considerably outside the boundary, indicating no significant trends except, as in the case at 425 K, at the outermost latitude bin. From this we conclude that there is no significant temporal trend at either level outside the boundary. The reevaluated data inside at 450 K are very consistent with the first evaluation, and both taken together indicate no significant temporal trend. In summary, within 5° latitude of the boundary, there is no significant temporal trend outside the boundary nor at 450 K inside the boundary, but there is a significant downward temporal trend of almost 20% inside the boundary at 425 K.

Figure 7 is a graphical representation of the N_2O isopleths relative to the boundary of the chemically perturbed region, with Figure 7*a* representing the conditions in late August and Figure 7*b* in late September. Where there are no significant trends (outside the boundary at both levels and inside at 450 K), the data in both Figures 7*a* and 7*b* are the averages taken from Figure 5. The 425 K data from inside the boundary are from the individual trend calculations, shown graphically in Figure 5, evaluated for August 23 and September 22. Virtually identical plots result from using the alternate trend calculations. The N_2O isopleths inside the boundary have steepened dramatically, indicating diabatic cooling during this period. In order to see this more clearly, consider the triangular portion of Figure 7*a* within the boundary and with N_2O mixing ratios between 130 and 140 ppbv. This area extends about 3° in latitude within the boundary at the 425 K

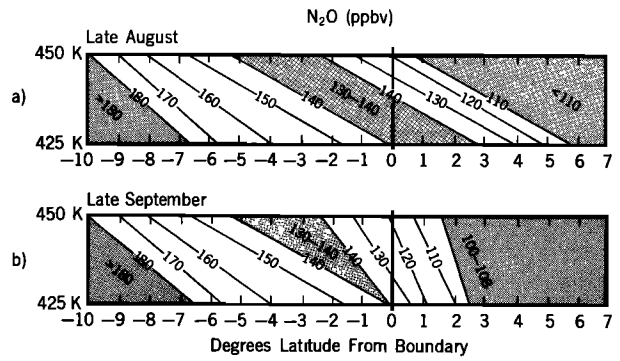

Fig. 7. N_2O isopleths from 425 to 450 K versus latitude relative to the boundary for (*a*) late August and (*b*) late September.

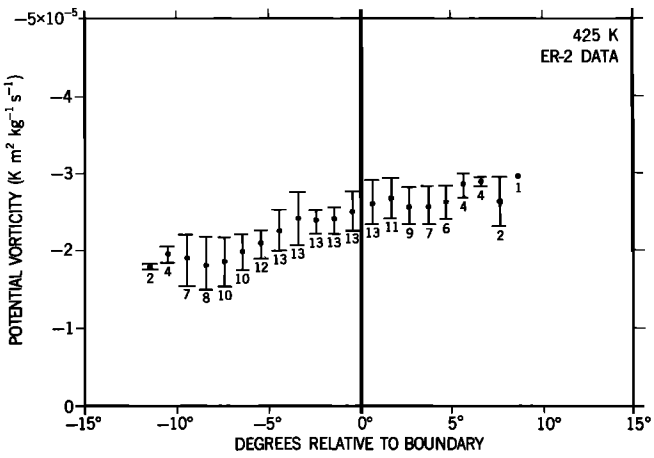

Fig. 8*a*

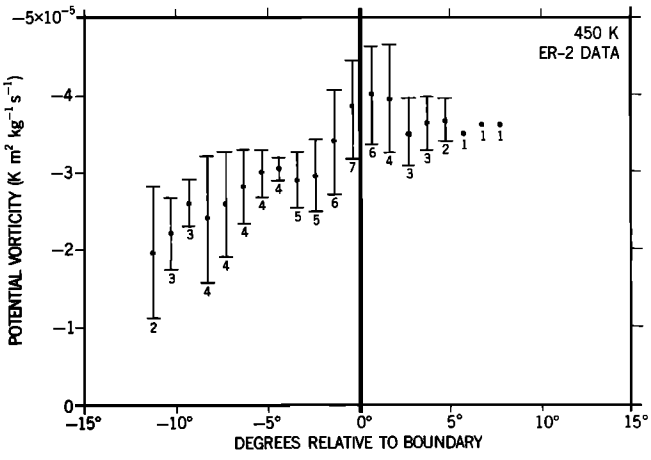

Fig. 8*b*

Fig. 8. Plots of averaged potential vorticity versus latitude referenced to the boundary of the chemically perturbed region (heavy vertical line) for the (*a*) 425 K and (*b*) 450 K flight levels. Data are averaged over 1° latitude intervals and over all flight data from August 23 through September 22 as in Figure 4 for N_2O.

level. However, in Figure 7*b* we see there is no air indicated within the boundary with a mixing ratio of 140 ppbv and only a very small triangle indicated over 130 ppbv. This displaced air has clearly cooled (descended) to lower potential temperatures. Here we would like to point out that this conclusion was reached by considering only the trends inside the boundary where both trend analyses are totally consistent. The lack of trends outside the boundary suggests a more stable situation there, but this does not necessarily mean there is no diabatic cooling. Quite to the contrary, the persistence of the steep inclination of the N_2O isopleths over a 1-month period, in the presence of latitudinal isentropic mixing which would tend to make the layer more homogeneous and create isentropic isopleths, implies ongoing diabatic cooling during this period. To ascertain the rate of diabatic cooling is more difficult to accomplish. By using Figure 7*a*, we can see that temporal trends in N_2O are not useful for calculating diabatic cooling rates even if we assume there is no mixing. This we can understand by considering an air parcel, we will call it Π, in late September at 425 K and 2° within the boundary (110 ppbv in Figure 7*b*). Although there was a decrease in N_2O during the preceding month of about 20% at that position, we can say little about the source of the air parcel Π. For example, in late August (Figure 7*a*), Π may have been at 425 K and 6° within the boundary, thereby undergoing no diabatic cooling whatsoever during the 1-month period. On the other hand, if Π undergoes precisely vertical descent during this period, it would require a cooling of about 15 K during the 1-month period. Clearly within the bounds of Figure 7*a* there are infinitely many solutions to this situation, all equally valid. To summarize, we cannot deduce the cooling rate from these data, but we do know there is ongoing diabatic cooling on both sides of the boundary. Cooling rates will be quantitatively evaluated later but only outside the boundary and in another context.

Potential Vorticity

The plots of daily potential vorticity at 65°W longitude on a grid of potential temperature versus latitude during the period of the mission [*Newman et al.*, 1988] indicate there are poleward decreases of potential temperature along potential vorticity isopleths with a slope of about 5 K for each degree of latitude near the boundary. On occasion, decreases of more than 50 K in a few degrees of latitude are seen in the meteorological data, often followed by increases occurring at 5°–10° in latitude inside the boundary. These features in potential vorticity are represented in Figure 1 where potential vorticity isopleths dip sharply within the boundary but at higher latitudes climb and become nearly isentropic. The potential vorticity gradients are also evident in Figure 8, which show potential vorticity along the isentropic ER-2 flight track analyzed similar to N_2O in Figure 4. The similarities between Figure 4 and Figure 8 graphically demonstrate that there are strong correlations between potential vorticity and N_2O. These correlations have also been demonstrated by *Schoeberl et al.* [this issue]. The temporal trends in potential vorticity with respect to the boundary, as given in Table 1, are consistent with the negative N_2O trends within the boundary, but also indicate negative trends outside and near the boundary that are not evident in the N_2O temporal trends. This discrepancy is probably due to the extended latitudinal averaging of more than 1° that is required to calculate potential vorticity. But in general we see the correlation also evident in the temporal trends.

It has been long established that potential vorticity can act as a conservative tracer under certain conditions. Correlation of potential vorticity with tracer species such as ozone, radioactivity, and carbon monoxide within folds that de-

velop near a jet has been reported many times in the literature [*Danielsen*, 1968; *Danielsen and Hipskind*, 1980; *Danielsen et al.*, 1970, 1987; *Browell et al.*, 1987]. Our observed correlations are further examples of such correlations and in a region undergoing diabatic cooling. The data can also be interpreted using *Ertel*'s [1942] potential vorticity theorem, which describes the necessary and sufficient conditions for a parcel of air to change its potential vorticity. Details of its derivation and guidance in its interpretation along with numerical examples demonstrating diabatic cooling of a parcel without changing its potential vorticity are presented by *Danielsen* [1989]. As presented by Danielsen, Ertel's theorem can be stated as follows: For a fixed air parcel a gradient of diabatic cooling (or heating) in the direction of the absolute vorticity vector is the only source or sink of potential vorticity for potential temperature surfaces that never meet the surface of the Earth. Clearly, the potential temperature surfaces considered here (above 400 K) satisfy this criterion, so Ertel's theorem applies to our data. Therefore, if diabatic cooling is uniform (that is, the gradient of the change in potential temperature is zero), there will be no change in potential vorticity. Also, if the cooling is not uniform but the gradient of cooling is orthogonal to the absolute vorticity vector, there will be no change in potential vorticity. Precise orthogonality of the two vectors is unlikely, since the direction of the absolute vorticity vector changes significantly when crossing the jet and always has both a vertical and a horizontal component. We conclude that within the precision of the measurements there is no evidence for a gradient in diabatic cooling. So the cooling can be characterized as spacially uniform during this period and during the period prior to the mission, when the gradients in potential vorticity and N_2O were established. However, cooling rates are needed to quantify the degree of uniformity.

Recently, *Haynes and McIntyre* [1987] have derived formulations from which they conclude, "There can be no net transport of Rossby-Ertel potential vorticity (PV) across any isentropic surface." This seems to imply that under all conditions, a parcel of air that has undergone diabatic change must also change its potential vorticity during that process. This would be inconsistent with our observation of air parcels undergoing diabatic cooling with no apparent change in potential vorticity. The problem here seems to be with what is meant by the word "transport," and according to McIntyre, the paper is consistent with our results. To perhaps help clarify our usage, we shall only mention that throughout this paper we are concerned primarily with movement (transport) of fixed air parcels without accounting for mixing with other air. For further clarification concerning this issue, the reader is referred to the definition of transport and flux in the beginning of section 2 of the Haynes and McIntyre paper (H. M. McIntyre, private communication, April 1989).

The isentropic gradients in potential vorticity seen in Figures 1 and 8 indicate restricted isentropic transport near the boundary on the scale of a few degrees of latitude. That is, large latitudinal isentropic transport requires a substantial change in potential vorticity except well within the boundary. Ertel's theorem precludes such transport without a change in potential temperature. Therefore only well within the boundary can such isentropic transport take place. Furthermore, in the small scale where the ultimate mixing occurs, the steep isentropic gradients indicate enhanced mixing of parcels of dissimilar origin. It is not the gradients that enhance mixing, but unless the gradients are maintained by transport, the mixing must decrease the gradients. Since the isentropic gradients did not decrease, there must be resupply of air by transport into the region. This resupply that is necessary to maintain these gradients in potential vorticity and N_2O, along with ongoing diabatic cooling, could only be characterized as a descending poleward flow across the boundary (see Figure 1). For if the transport were northward across the boundary, it would require diabatic heating of the air or a change in its potential vorticity, both contrary to previous arguments. The obvious result of this poleward flow is ozone-rich stratospheric air being transported into the ozone hole.

POLEWARD TRANSPORT

The relative importance of poleward versus equatorward transport of air across the boundary is what we address in this section. We rely heavily on interpretation of the NO_y versus N_2O scatter plots to show there is little outward transport and mixing evident at flight altitudes, showing less than 10% of the air outside the boundary was processed within the boundary. We also consider the potential vorticity, total water, and ozone data in our analysis.

The sum of the reactive nitrogen species (NO_y) was observed to be very low within the boundary but not outside the boundary [*Fahey et al.*, this issue]. Figures 9*a* and 9*b* show NO_y versus N_2O data that have been binned for 425 ± 10 K and 450 ± 10 K, then averaged over the seven flights where NO_y was measured. Data taken when particles were present were excluded in order to obtain only gas phase NO_y [*Fahey et al.*, 1989]. Figure 9*a* includes all such data, while Figure 9*b* includes only data outside the boundary along with a linear least squares fit to the data. Excluded from that fit are the three points at the lowest N_2O values (two from 425 K and one from 450 K) that are somewhat below the fit. The differences between Figures 9*a* and 9*b* at the highest values of NO_y are due to the flight-to-flight movement of the boundary relative to the N_2O isopleths. Figure 9*c* includes experimental data and model calculations. The two data points in the figure indicated as "balloon" measurements were taken during October 1979 at 34°S [*Galbally et al.*, 1986] where NO_y is the sum of HNO_3, NO_2, and NO. Since this does not include all of the reactive nitrogen species (N_2O_5 and $ClONO_2$ being the notable exceptions), the value are perhaps 10% low. The points indicated as "model" calculations are from a one-dimensional radiative convective photochemical model for mid-latitudes at equinox [*Brasseur and Solomon*, 1986]. Also included are data taken on October 3 during the northbound ferry flight of the ER-2 between Panama City and NASA Ames Research Center in Moffett Field, California. The straight line fit to the data in Figure 9*b* is also included. Note that the straight lines indicated in the figure are nearly parallel, with the model predicting this photochemically driven partitioning to be linear up to values for NO_y of 14 ppbv. An offset of 25–50 ppbv is indicated between the ATLAS ER-2 data and both the balloon data and the model calculation. This is similar to the 30 ppbv offset mentioned earlier between the ATLAS measurements and the whole-air samples taken simultaneously on the ER-2. We conclude from Figures 9*a* and 9*c* that denitrifica-

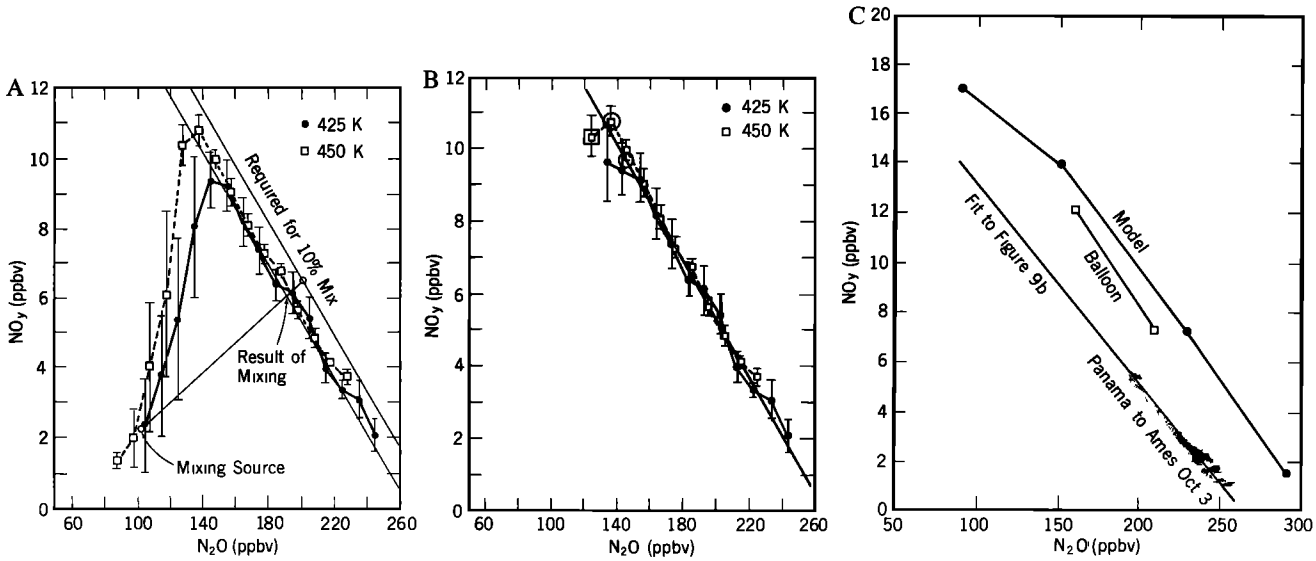

Fig. 9. (*a*) NO_y versus N_2O binned for the 425 and 450 K flight levels and averaged over the seven flights where data were available. Data taken during particle events (PMS > 300) were excluded in order to obtain only gas phase NO_y. Linear least squares fit to data as in Figure 9*b* and an example of outward mixing are also included. (*b*) As in Figure 9*a* but only includes data outside the boundary. Straight line is linear least squares fit to the data excluding the two points at 425 K and one point at 450 K at lowest values for N_2O (see text). (*c*) NO_y versus N_2O plot of (1) the linear least squares fit to the data of Figure 9*b*, (2) the data taken on the return ferry flight of the ER-2 between Panama City and Moffett Field, California, (3) data taken at 34°S from a balloon payload [*Galbally et al.*, 1986], and (4) a mid-latitude model calculation [*Brasseur and Solomon*, 1986].

tion within the boundary causes the low values of NO_y within the boundary, and from Figures 9*b* and 9*c* that data taken for NO_y and N_2O outside the boundary are in excellent agreement with the data taken on October 3 and, except for an offset, in agreement with mid-latitude balloon data and model calculations.

It has been previously stated that the boundary restricts equatorward transport at these potential temperatures (425 and 450 K). For if there were such transport, low values of NO_y, total water, and ozone found inside the boundary would be expected to be common outside of the boundary as well, unless very rapid mixing was also occurring. If there were rapid mixing, it would tend to round the sharp latitudinal gradients at the boundary that are observed in many constituents but most notably ClO, NO_y, and ozone [*Proffitt et al.*, 1989]. Figure 9*a* indicates a slight rounding of NO_y when plotted against N_2O, but we will consider only data from outside the boundary, where a more detailed analysis can be made. There are only three points at low N_2O values that deviate from the straight line fitting the rest of the data, and these alone indicate the outward transport across the boundary. However, on the last Antarctic flight date, September 22, there was a clear indication of the movement of air northward across the boundary penetrating about 3° of latitude and seen as low values of N_2O , NO_y, total water, and ozone at 425 K [*Tuck*, 1989]. As discussed above, this is as expected from outward transport without rapid mixing. Only on this flight did such an event occur, as is demonstrated in Figure 9*b*. The data comprising the three points that deviated from the straight line were again calculated by deleting the data from September 22. These three new points are plotted in Figure 9*b* as two open circles (425 K) and as a large open square (450 K). The two points at 425 K, where the event was observed on September 22, now lie near the straight line fit, but the other point at 450 K, as expected, did not change and still deviates slightly from the fit. Therefore it appears that September 22 is the only flight day on which there is evidence of large-scale outward transport across the boundary at 425 K. Clearly this is not an indication of outward flow that had persisted during the mission. Although this may appear to indicate outward mixing, we feel that it is more likely to indicate the first phase of incorporation of air from outside the boundary into the vortex. This requires a parcel of unprocessed air peeling off poleward and appearing to isolate the parcel of processed vortex air we observed on September 22. This is then simply an observation of the general poleward flow of air into the vortex. The high wind shear near the boundary could next strip the unprocessed parcel into thin ribbons and effectively promote it being mixed into the vortex. Another possibility is that the unprocessed parcel may move poleward where isentropic mixing is enhanced. There is evidence of this process occurring throughout the mission both in the large-scale United Kingdom Meteorological Office potential vorticity plots [*Tuck et al.*, 1989*b*], and, on a much smaller scale, through correlations of trace species. The region where this process of peeling off and incorporation into the vortex occurs is the same as the transition region referred to elsewhere [*Murphy et al.*, 1989; *Tuck*, 1989]. These data contain little evidence for sustained northward transport or mixing across the boundary.

Another interpretation of the September 22 data is presented elsewhere using forecast isentropic trajectory analysis [*Tuck*, 1989] to indicate removal of air from the interior of the vortex, showing transport across the vortex to 51°S in about 4 days. Whether there is some transport out of the

vortex to lower latitudes is not the question addressed here, and we do not consider the calculated trajectory to be inconsistent with our basic conclusion. However, using either the forecast analysis or the assimilation analysis (where fields are adjusted to fit meteorological observations) for potential vorticity at 428 K (-3.0×10^{-5} K m^2/kg s), the general direction of flow is indicated to be poleward across the boundary. This is evident in the frequent occurrence of contours of potential vorticity characteristic of the boundary region protruding well into the vortex and often becoming disconnected from the boundary contour. The relatively rare occurrence of such great extensions and disconnected contours outside the boundary indicates that outward flow is not important (see several figures showing potential vorticity in *Tuck* [1989]), again supporting the conclusion reached in the previous paragraph.

In order to quantitatively evaluate the degree of possible outward mixing across the boundary, we have plotted a line in Figure 9*a* that represents the NO_y-N_2O combinations that when mixed in a 9 to 1 ratio with air from 5° within the boundary would result in our measured linear relationship. That line is labeled "required for 10% mix," and the source for the mix is labeled as "mixing source." This line was calculated so that the result of mixing the mixing source to a 10% level with any point on the required for 10% mix line would result in the point common to the straight line connecting those two points and the straight line fit to the original data.

Using Figure 9*a* as a guide, we now establish the following: if during the mission there was ongoing outward mixing of air from 425 to 450 K that originated 5° within the boundary, then that processed air would compose less than 10% of the mixture at any position outside the boundary and along our flight tracks. In Figure 9*a*, our hypothetical mixing source of processed air within the boundary is shown along with an example of the result of 10% mixing of that source with a combination of NO_y and N_2O that will reproduce the measured data. We can see that in order for the result of the mixing process to lie within the variability of the measured data, it must be mixed with air that does not lie within the measured variability. All measured data either inside or outside the boundary were found to be consistent with the linear fit of the 425 and 450 K data in Figure 9*a*, or else it was denitrified. Now let us suppose that air sampled outside the boundary at 425–450 K (indicated as "result of mixing" in Figure 9*a*) is composed of at least 10% air from 5° within the boundary that was also at 425–450 K ("mixing source" in Figure 9*a*). If that 10% were removed from the parcel, the resulting parcel would lie on the "required for 10% mix" line. Statistically, we did not observe such a parcel; therefore a source of air outside of our sampled region is required to obtain a mix that is consistent with our data. We now search for such a source. First we will consider air that has a potential temperature lower than 425 K. As depicted in Figure 1, the lower potential temperatures were sampled on every flight, not only on ascent and descent at 53°S but also within the boundary at 72°S. Since the boundary covered a wide latitude range (59°–71°), our sampling at fixed latitudes represents a large sampling of the region. As we stated, no sampled data would be suitable for our "required" source, so out to at least 53°S, no low potential temperature source is suitable. Next we search above 450 K. Here we have few data, so we cannot rule out such mixing at these high potential temperatures. But we can exclude the possibility of the mixing occurring at 425–450 K by considering the variability in the data in Figure 9*a*. That is, the variability indicated by the vertical bars does not intersect the required line as we would expect if this were where the mixing occurred. However, if our hypothetical mixing source at 425–450 K were being mixed into air above 450 K, this would require our source to be diabatically heated. Since we have established diabatic cooling is taking place in this region, we can eliminate this possibility. Therefore there is no suitable source of air at our flight level, below our flight level, or above our flight level, at least over the latitude range covered on our flights. So our supposition cannot be true that the air sampled outside the boundary at 425–450 K is composed of at least 10% air from 5° within the boundary and at a potential temperature of 425–450 K. We conclude that there is no evidence for outward mixing of air across the boundary at 425–450 K. Of course, we have no information regarding the possible outward mixing at the higher potential temperatures unless we assume that such air descended into our sampled region. But if the air sampled outside at 425–450 K were partly composed of inner vortex air, mixing must have occurred above our flight altitudes with the resulting air then appearing at flight altitudes as unprocessed, i.e., NO_y normal relative to N_2O and ozone showing no sign of large temporal decrease. This is not impossible but seems unlikely. The outward transport and mixing most likely occur below 425 K as indicated in Figure 1.

Total water data taken during ascent and descent out of Punta Arenas have been interpreted as indicating vortex-processed air near 53°S. Water mixing ratios of 2.5–3.0 ppmv during the first 2 or 3 weeks of the mission [*Kelly et al.*, 1989] are consistent with inner vortex air. The lowest values reached during this period were from 2.2 (August 28 only) to 2.4 ppmv. With one notable exception, that being August 23, these low values over Punta Arenas occurred below 425 K. Plausible explanations for these low mixing ratios can be made without directly transferring air from inside the vortex to 53°S. Two events are used to support this view. First, during the ER-2 ferry flights during August, low water mixing ratios were observed as follows: (1) August 12 at 14° N and 450 K, mixing ratio of 2.4 ppmv, (2) August 14 continuous low values from 10°S to 25°S and 425 to 450 K with mixing ratios from 2.6 to 2.8 ppmv, and (3) August 15 at 42°S and 350 K, mixing ratio of 2.5 ppmv. This does not imply that these are the lowest values at any altitude, only that in the normal course of the flights these low values were found commonly and over a wide range of latitudes in the southern hemisphere. Second, from the meteorological wind cross sections [*Newman et al.*, 1988], there appears to be a rapid movement of the southern hemisphere subtropical jet from its usual 30°S latitude on August 18 to about 60°S on August 23. This could have the effect of rapidly transporting low-latitude dehydrated air, such as were observed on the ferry flights a few days earlier, into the region over Punta Arenas. Supporting this hypothesis is the observation that August 23 was the only day we observed water mixing ratios near Punta Arenas below 2.7 ppmv with a potential temperature of 425 K or above. On August 23, mixing ratios of 2.4–2.5 ppmv from 350 to 450 K were observed. From the observations on August 14 at 450 K we can see that the air observed from 15°S to 25°S is consistent with the air observed over Punta Arenas on August 23. It is our opinion

that these observations present a plausible explanation for the low water mixing ratios observed in the 425–450 K range without outward mixing from within the vortex. Similar observations in the data below 400 K, by considering the data of August 15 at 42°S, imply that the still lower values (down to 2.2 ppmv) on August 23 and August 28 may also have come from the north rather than the south. We do not mean to rule out outward transport as a partial explanation for the low mixing ratios below 400 K, but only to offer an alternate explanation in the absence of proof of direction of flow. Indeed, with the descending poleward flow at 425–450 K that we have established in this paper, there must be an outflow toward the north at some level. The outflow is shown in Figure 1 as north pointing arrows between about 300 and 400 K. As support for the equatorward transport of vortex air at these lower potential temperatures are measurements made from the DC-8, well below the flight altitudes of the ER-2. In particular, *Kelly et al.* [1989], *Gregory et al.* [this issue], and *Tuck* [1989] report from in situ water and ozone mixing ratios at the DC-8 flight level of about 315 K, that below the boundary of the chemically perturbed region, there was a band about 10° in latitude wide of low water mixing ratios and high ozone mixing ratios when compared with the regions either side of that band. This could imply that the higher ozone and lower water mixing ratios found at the higher potential temperatures within the chemically perturbed region had descended to DC-8 altitudes. Lidar data (ozone and aerosol) also indicated this region to occasionally show a definite "fold" or "tongue" of high ozone air and is discussed by *Tuck* [1989]. This interpretation is consistent with the diabatic poleward descent we have described.

Temporal trends in ozone have also been used to support the lack of outward flow across the boundary [*Proffitt et al.*, this issue]. By considering ozone temporal trends on isentropic surfaces inside and outside the boundary, negative temporal trends of −44% to −62% with small residuals were found inside, but outside and near the boundary where we should see the largest effect of outward transport, no significant change in ozone was found. The small negative trends (−16% and −19%) at 450 K with residuals comparable to the trends are due to the high ozone measured outside the boundary at this level on August 23 when the flight track was unusually high and the potential temperature was above 460 K. Due to the lack of data and the scatter of the data available, these trends were not considered significant in that paper. In summary, we see that from the NO_y and N_2O data, the United Kingdom Meteorological Office potential vorticity calculations, the total water data over Punta Arenas and the ozone temporal trend data, there is no convincing evidence to support significant large-scale outward transport across the boundary at 425 and 450 K, except perhaps on September 22, the last day of our mission. Indeed, the NO_y versus N_2O data and the ozone temporal trends are inconsistent with such transport.

Advective Flow and Mixing Near the Boundary

We have speculated that the poleward diabatically descending air is predominantly advective rather than dispersive. Advection describes the bulk movement of air masses, in some organized fashion, without diffusive spreading into the surrounding environment. Examples of advection are the winds, reversible wave activity, and the expansion or contraction and sinking or rising due to changes in temperature and pressure. Conversely, dispersion describes the disorganized irreversible processes that mix different air masses down to the molecular scale. Examples of mixing all ultimately reduce to molecular diffusion, but only after many advective processes have interspersed those masses finely enough that the molecular diffusion can be effective. Therefore, through dispersion, quite dissimilar air masses can be mixed, forming a homogeneous mass that shares the character of its original constituents. For example, parcels from high altitudes can be brought down to lower altitudes by large-scale waves and then interspersed with the lower altitude air on a finer and finer scale also by waves until molecular diffusion effectively mixes the original components irreversibly. A characteristic of dispersion is that it smooths out gradients in atmospheric constituents through mixing, while advection alone does not. Advection can create gradients by moving dissimilar air parcels near one another. Both advection and dispersion simultaneously play a role in atmospheric transport, so what we observe in the atmosphere is a combination of both processes. We will now present evidence showing that our observations in the Antarctic near the boundary of the chemically perturbed region indicate dominantly advective poleward transport across the boundary at and above 425 K, with a mixing region within the boundary extending well below the flight level of the ER-2. A concurrent flow into the mixing region from the interior of the vortex is also indicated.

We have shown in previous sections that air is diabatically cooled and transported poleward across the boundary. The cooling process produces descending air with a vertical component, and the poleward transport that is derived from the data requires a horizontal component. The gradients seen in Figures 4 and 8 could be produced from vertically descending air being mixed with horizontally transported air. This describes a dispersive rather than advective process from the north. However, Figure 7 indicates a steepening and therefore narrowing of the isopleths in N_2O near the boundary as the mission progressed. This contrasts the broadening or smoothing of the gradients expected from a dispersive process. Therefore Figure 7 indicates the transport is dominantly advective near the boundary. The narrowing of the isopleths due to the compression of the advective descent can also be seen here and in Figure 8 of *Podolske et al.* [this issue]. We have now established that since the poleward diabatically driven descent is advective, the transport must be along the lines of constant N_2O and potential vorticity.

Further interpretation of Figures 4, 7, and 8 inside the boundary can also be made. First note that the general character of Figures 4 and 8 is a decrease when approaching the boundary from the north, steepening at the boundary, then a leveling off or slight increase up to about 2°–6° within the boundary, followed by a resumed decrease. This region from the boundary and up to 6° inside is where the "ozone trench" was observed in the ER-2 in situ ozone data [*Proffitt et al.*, this issue] and is where the "collar" region was described from observations made on the DC-8 of enhanced column measurements of $ClONO_2$ and HNO_3 [*Toon et al.*, this issue]. If in this region of strong diabatic descent, the poleward flow across the boundary is met by a northward

flow from within the vortex, it would produce a mixing region of descending air that would reflect the character of the interior of the vortex as well as the region near the boundary. Our data support this hypothesis. The leveling off described above in Figures 4 and 8 indicates a region of dispersion (smoothing of gradients) that contrasts the steep slopes at the boundary where advection is the dominant characteristic. In Figure 1 we indicate transport of air from within the vortex by the north pointing arrows at the right of the figure and the region of confluence (ozone trench) at 70°S. There are insufficient data from the ER-2 to say more about what occurs beyond 6° within the boundary.

We now conclude that there is dominantly advective poleward transport across the boundary at and above 425 K along constant N_2O and potential vorticity isopleths, matched by concurrent northward transport from within the vortex, into a mixing region that extends down to at least 315 K.

DIABATIC COOLING RATE

Plots of total water versus latitude relative to the boundary for three of the 10 flights during this period are shown in Figure 10. The nonuniformity of the dehydration within the boundary and the uniformly high values outside the boundary can be seen in the figure and are characteristics found on every flight [*Kelly et al.*, 1989]. All ER-2 flights showed water mixing ratios over 3.2 ppmv inside the boundary, but they often dropped to less than 2.0 ppmv. The higher values were usually within a few degrees latitude of the boundary. Data in Figure 10 show typical water mixing ratios outside the boundary that remain high well into the chemically perturbed region. This appears to require a resupply of water from outside the boundary and is consistent with the poleward transport across the boundary that we have already established.

Temporal trends in total water were calculated in the same manner as discussed earlier for N_2O (Table 1). Since we do not have a well-defined potential temperature dependence for total water mixing ratios, the alternate method used for N_2O in Table 1 could not be applied. For the 5° of latitude outside the boundary, the trends varied from +11% to +19% with residuals of about 3% [*Proffitt et al.*, 1989]. Figure 11 shows the data from the trend calculations near the boundary and the linear fit to the data. There is a clear upward trend in water with little scatter in the data. This upward trend in water reflects the variability we observed at other latitudes. For example, on the ferry flight of September 29, a change in water mixing ratios from 3.3 to 4.0 ppmv was observed when flying from 43°S to 48°S at a potential temperature of 480 K. The poleward progression of such mid-latitude air would be seen as an increasing temporal trend in our analysis near the boundary.

The observed upward temporal trend is further evidence in support of our previous conclusion that there is little if any outward transport from within the boundary at these potential temperatures. This can be seen by considering the temporal trends in water at 425 K within the boundary as presented by *Proffitt et al.* [1989] and shown in Table 1. These trends range from no significant temporal trend 1° within the boundary, to negative trends of 13–42% for the next 4°, averaging almost 30%. These trends are dominated by decreases in water before September 16, at which time

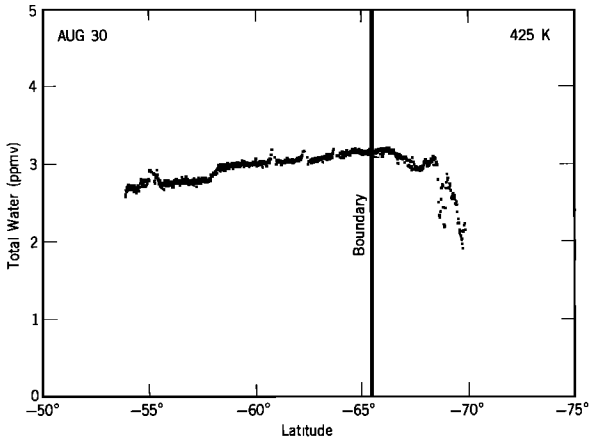

Fig. 10*a*

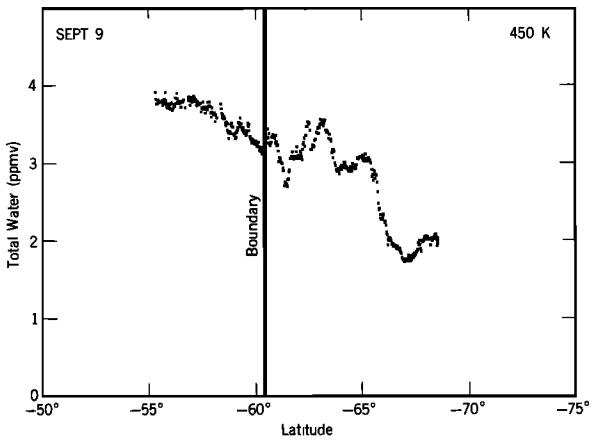

Fig. 10*b*

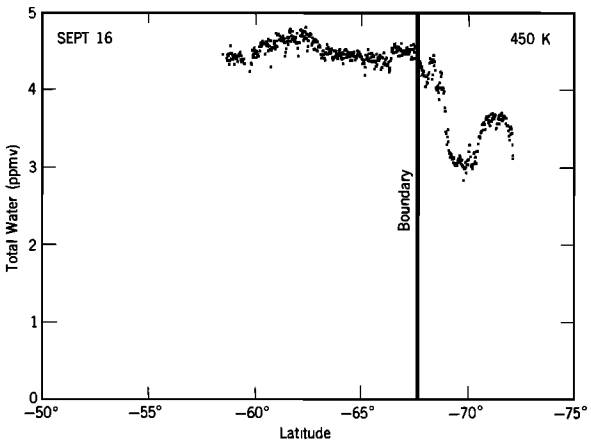

Fig. 10*c*

Fig. 10. Total water mixing ratios versus latitude on (*a*) August 30 at 425 K, (*b*) September 9 at 450 K, and (*c*) September 16 at 450 K. The boundary of the chemically perturbed region for those particular flight legs is indicated with heavy vertical lines.

the dehydration within the vortex had effectively stopped [*Kelly et al.*, 1989]. But temporal increases were not seen within the boundary even during these later flights except near the boundary (these increases were due to air that crossed the boundary with higher water content). Therefore we can see that the increasing water outside the boundary does not match the decreasing temporal trends seen within the boundary. We again conclude that the temporal trends

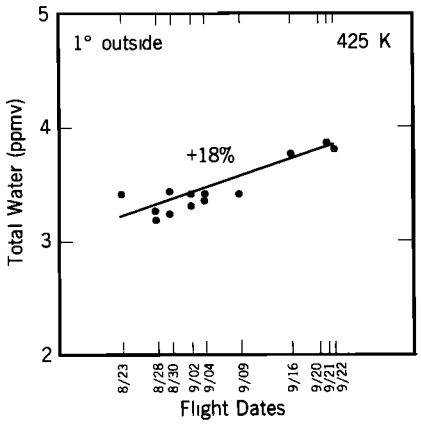

Fig. 11*a*

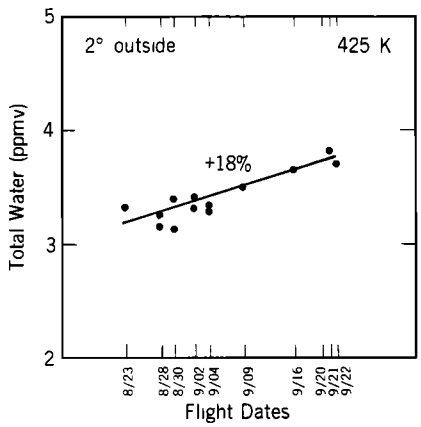

Fig. 11*b*

Fig. 11. Total water temporal trends at 425 K at (*a*) 1° and (*b*) 2° latitude outside of the chemically perturbed region.

seen in Figure 11 cannot be due to outward isentropic transport.

We have established that there is a general downward diabatic flow of air along the constant N_2O isopleths shown in Figure 7. Therefore an air parcel outside the boundary at 450 K late in August should eventually cross the 425 K surface. Since the N_2O isopleths with values greater than 140 ppbv do not change during this 1-month period, we can see that as long as we choose N_2O to be greater than 140 ppbv, we can track a parcel that begins at 450 K along its descent to 425 K by following the appropriate isopleth in either Figure 7*a* or 7*b*. This cannot be done for N_2O less than 140 ppbv, since those isopleths may end up across the boundary where the slopes are changing during the 1-month period. In particular, if the descent took a month or less, Figure 7*b* indicates that a parcel near the boundary at 425 K in late September would have been 3°–6° outside the boundary at 450 K some time during the previous month. This particular path will be used in our calculation of a diabatic cooling rate.

Table 2 contains average values of total water for six different flight days and various positions outside the boundary. Except for August 23, the data are all within the 450 K bin, but the potential temperatures indicated for August 23 again reflect the difficulty in using these data for temporal trends. Here we consider the August 23 mixing ratios as indicating initial low values at the 450 K level of no more than 3.4 ppmv.

Now we will determine the time required to descend from 450 to 425 K by comparing the data far out from the boundary in Table 2 with the data near the boundary and at 425 K in Figure 11, thereby following the N_2O isopleths in Figure 7*b*. Consider an air parcel, as indicated in Table 2 on August 23, with a mixing ratio of no more than 3.4 ppmv. The data shown in Figure 11 indicate that the mixing ratio on the 425 K level increased to 3.4 ppmv during the 2 weeks following August 23. Similarly, an air parcel on September 9 (Table 2) with a mixing ratio of 3.8 ppmv would be indicated to arrive again about 2 weeks later near the boundary and at 425 K (Figure 11). Although this interpretation depends on data from the two flights of August 23 and September 9, the consistency of the data set seems to warrant such a detailed examination. So we conclude in both cases, that there is diabatic descent from 450 to 425 K in about 2 weeks, requiring an average cooling rate of 1.75 K per day in potential temperature during the entire 1-month period. This corresponds to a descent of about 100 m/d.

ANGULAR MOMENTUM BUDGET

We stated in the introduction that the boundary is located slightly to the poleward side of the maximum wind speed of the polar jet as observed on an isentropic surface. In the absence of frictional losses or mixing with air of a lower angular momentum, the angular momentum of a parcel will not change, so if that parcel is moved poleward, the wind speed must increase to compensate for the change in latitude. Therefore our observations of a simple advective poleward flow across the boundary must be accompanied by either frictional losses, mixing with air of lower angular momentum, or an increase in wind speed.

TABLE 2. Total Water Mixing Ratios

Degrees Relative to Boundary	Aug. 23	Average Potential Temperature for Aug. 23, K	Sept. 9	Sept. 16	Sept. 20	Sept. 21	Sept. 22
−6	3.2	489		4.3	4.1	4.1	4.0
−5	3.4	485		4.3	4.0	4.1	4.0
−4	3.4	482	3.8	4.2	4.0	4.1	3.9
−3	3.5	479	3.9	4.1	4.0	4.1	4.0
−2	3.5	470	3.8	4.1	4.1	4.1	4.0
−1	3.5	464	3.5	4.2	4.1	4.1	3.7

All mixing ratios averaged over potential temperature bin from 440 to 460 K except data from August 23. Blanks indicate no data were available. Unit of measure is ppmv.

Changes in a parcel's angular momentum due to interaction with the surface of the Earth (frictional forces) is believed to be significant when considering the angular momentum budget of the atmosphere [*Swinbank*, 1985]. The average latitude for the location of the boundary is 66°S [*Proffitt et al.*, 1989], which is approximately the latitude at which an air parcel, spiraling toward the pole on a trip within the polar jet, would first encounter significant orographic perturbation from the Antarctic continent. Therefore the change in angular momentum we observe may be accounted for, at least in part, by orographic effects.

In the previous section we showed that there is a region where the poleward moving air (possessing high angular momentum) is mixed with air from well within the boundary (possessing low angular momentum). This will also produce a decrease in angular momentum as we proceed poleward through the mixing region.

Perhaps the most important contribution to balancing the angular momentum budget results from the observed temporal change in wind speed over the mission. A 1-month increase in wind speed that averaged 73% was observed for the first 5° within the boundary at 425 K [*Proffitt et al.*, 1989]. As previously discussed, this large increase is reasonable when we consider the angular momentum of a parcel that is descending and moving poleward across the boundary. The descending component would require an increase in wind speed (the jet is stronger above), and the poleward component would do the same by the change in latitude. The combined effect of orographic decreases due to the Antarctic continent, the outward mixing of low angular momentum air from within the vortex, and the observed temporal behavior of the wind speed could easily balance the angular momentum budget on the poleward side of the jet.

SUMMARY AND CONCLUSIONS

From N_2O, total water, total odd nitrogen (NO_y), and potential vorticity, we have presented a consistent picture of dominantly advective poleward movement of air across the boundary at and above 425 K matched by a concurrent northward flow from within the vortex, into a mixing region extending down to at least 315 K. We found little evidence for significant transport of air in the reverse direction across the boundary at these potential temperatures, although at 300–400 K there is some evidence supporting transport out of the vortex to lower latitudes. This equatorward transport may be within the stratosphere and could be the return leg for the poleward flow we describe between 425 and 450 K.

We summarize our finding again using Figure 1. Here we see the result of diabatic cooling and confluence of air at the polar jet. Near the polar jet and above 400 K, the potential vorticity isopleths indicate the diabatic flow pattern, and the arrows give the direction of the flow. The region centered at about 70°S and below about 400 K, where these isopleths dip sharply, show the combined result of diabatic cooling and the confluence of air from both sides of the polar jet. This region also corresponds to the "ozone trench" and the "collar" referred to elsewhere in this issue. Also in this region but below about 400 K, there is descent and significant turbulent mixing. As the descending air then proceeds toward the north, the ozone-depleted, dehydrated, and denitrified air that descended through the chemically perturbed region mixes with unprocessed air. Although this unprocessed air might have been dehydrated over Antarctica, the dehydration apparently took place well below the region of ozone loss. In situ ozone, in situ total water, and ozone lidar measurements, all made from the DC-8 flying at about 315 K, indicate the outflow of vortex air to be at latitudes corresponding to about 5° on either side of the boundary.

Outside the region of steep gradients in potential vorticity, we see isopleths become nearly parallel to the potential temperature surfaces, indicating enhanced isentropic transport. From this, we suggest that the general circulation from mid-latitudes toward the pole is diabatically driven by cooling that intensifies near the jet. This intensification is centered at the boundary of the chemically perturbed region and at the average latitude of the edge of the Antarctic continent, where surface radiation drops abruptly. Large-scale isentropic transport becomes less and less important as we approach the jet, where diabatic cooling intensifies and the steeply inclined potential vorticity isopleths inhibit isentropic transport. Here small-scale turbulent mixing becomes more efficient. Well within the vortex, the isopleths again become nearly parallel to the potential temperature surfaces, and large-scale isentropic transport can again occur.

How much air is returned into the troposphere rather than into the stratosphere is not clear from the data presented. Since the air in this region is moving rapidly around the pole with a round trip taking about 1 week, it is conceivable that the return leg of the flow pattern indicated is not at the longitude of our observations. Satellite data have been presented that suggest just such an asymmetric flow [*Watterson and Tuck*, this issue]. However, regardless of the return path, the impact of the processing of air within the ozone hole is increased by the dynamic model we have presented.

To summarize our primary data analysis, we feel we have established the following results for air near the boundary and at potential temperatures from 425 to 450 K.

1. N_2O temporal trends indicate that diabatic cooling occurs both inside and outside the chemically perturbed region.
2. Potential vorticity is conserved in air parcels undergoing diabatic cooling, and this implies that the cooling is uniform.
3. N_2O, potential vorticity, and water data reveal an advective poleward flow of air across the boundary.
4. There is no significant large-scale outward transport across the boundary at 425–450 K.
5. There is a mixing region within the boundary that extends down to at least 315 K.
6. Water temporal trends give diabatic cooling rates outside the boundary of 1.75 K per day in potential temperature.
7. These results are consistent with the angular momentum budget in this region.

Acknowledgments. The authors are very grateful to Ed Danielsen for his encouragement and many stimulating and helpful discussions. We also express our thanks to Mark R. Schoeberl for the use of his potential vorticity calculations. Full support for the travel associated with the Airborne Antarctic Ozone Experiment was provided to the Aeronomy Laboratory by the Chemical Manufacturers Association. Partial support for the development and construction of the apparatus used by the Aeronomy Laboratory had been provided earlier by the National Aeronautics and Space Administration as part of the Stratosphere-Troposphere Exchange Project conducted in the winter of 1987.

REFERENCES

Anderson, J. G., W. H. Brune, and M. H. Proffitt, Ozone destruction by chlorine radicals within the Antarctic vortex: The spatial and temporal evolution of ClO-O_3 anticorrelation based on in situ ER-2 data, *J. Geophys. Res.*, *94*, 11,465–11,479, 1989*a*.

Anderson, J. G., W. H. Brune, S. A. Lloyd, W. L. Starr, M. Loewenstein, and J. R. Podolske, Kinetics of O_3 destruction by ClO and BrO within the Antarctic vortex: An analysis based upon in situ ER-2 data, *J. Geophys. Res.*, *94*, 11,480–11,520, 1989*b*.

Brasseur, G., and S. Solomon, *Aeronomy of the Middle Atmosphere*, 2nd ed., D. Reidel, Hingham, Mass., 1986.

Browell, E. V., E. F. Danielsen, S. Ismail, G. L. Gregory, and S. M. Beck, Tropopause fold structure determined from airborne lidar and in situ measurements, *J. Geophys. Res.*, *92*, 2112–2120, 1987.

Danielsen, E. F., Stratospheric-tropospheric exchange based on radioactivity ozone and potential vorticity, *J. Atmos. Sci.*, *25*, 502–518, 1968.

Danielsen, E. F., A note in defense of Ertel's potential vorticity and its general applicability as a meteorological tracer, *J. Atmos. Sci.*, in press, 1989.

Danielsen, E. F., and R. S. Hipskind, Stratospheric-tropospheric exchange at polar latitudes in summer, *J. Geophys. Res.*, *85*, 393–400, 1980.

Danielsen, E. F., R. Bleck, J. Shedlovsky, A. Wartburg, P. Haagenson, and W. Pollock, Observed distribution of radioactivity, ozone, and potential vorticity associated with tropopause folding, *J. Geophys. Res.*, *75*, 2353–2361, 1970.

Danielsen, E. F., R. S. Hipskind, S. E. Gaines, G. W. Sachse, G. L. Gregory, and G. F. Hill, Three-dimensional analysis of potential vorticity associated with tropopause folds and observed variations of ozone and carbon monoxide, *J. Geophys. Res.*, *92*, 2103–2111, 1987.

Ertel, H., Ein neuer hydrodynamischer wirbelsatz, *Meteorol. Z.*, *59*, 277–281, 1942.

Fahey, D. W., K. K. Kelly, G. V. Ferry, L. R. Poole, J. C. Wilson, D. M. Murphy, M. Loewenstein, and K. R. Chan, In situ measurements of total reactive nitrogen, total water, and aerosol in a polar stratospheric cloud in the Antarctic, *J. Geophys. Res.*, *94*, 11,299–11,315, 1989.

Fahey, D. W., D. M. Murphy, C. S. Eubank, K. K. Kelly, M. H. Proffitt, G. V. Ferry, M. K. W. Ko, M. Loewenstein, and K. R. Chan, Measurements of nitric oxide and total reactive nitrogen in the Antarctic stratosphere: Observations and chemical implications, *J. Geophys. Res.*, this issue.

Galbally, I. E., C. R. Roy, R. S. O'Brien, B. A. Ridley, D. R. Hastie, W. F. J. Evans, C. T. McElroy, J. B. Kerr, R. A. Plumb, P. Hyson, and J. E. Laby, Trace constituents in the austral stratosphere, *Q. J. R. Meteorol. Soc.*, *112*, 775–809, 1986.

Gregory, G. L., W. D. Hypes, L. S. Warren, A. F. Tuck, K. K. Kelly, and A. J. Krueger, Tropospheric ozone in the vicinity of the ozone hole: 1987 Airborne Antarctic Ozone Experiment, *J. Geophys. Res.*, this issue.

Hartmann, D. L., K. R. Chan, B. L. Gary, M. R. Schoeberl, P. A. Newmann, R. L. Martin, M. Loewenstein, J. R. Podolske, and S. E. Strahan, Potential vorticity and mixing in the south polar vortex during spring, *J. Geophys. Res.*, *94*, 11,625–11,640, 1989.

Hartmann, D. L., L. E. Heidt, M. Loewenstein, J. R. Podolske, J. Vedder, W. L. Starr, and S. E. Strahan, Transport into the south polar vortex in early spring, *J. Geophys. Res.*, this issue.

Haynes, P. H., and M. E. McIntyre, On the evolution of vorticity and potential vorticity in the presence of diabatic heating and frictional or other forces, *J. Atmos. Sci.*, *44*, 828–841, 1987.

Heidt, L. E., J. F. Vedder, W. H. Pollock, R. A. Lueb, and B. E. Henry, Trace gases in the Antarctic atmosphere, *J. Geophys. Res.*, *94*, 11,599–11,611, 1989.

Kelly, K. K., et al., Dehydration in the lower Antarctic stratosphere during late winter and early spring 1987, *J. Geophys. Res.*, *94*, 11,317–11,357, 1989.

Murphy, D. M., A. F. Tuck, K. K. Kelly, K. R. Chan, M. Loewenstein, J. R. Podolske, M. H. Proffitt, and S. E. Strahan, Indicators of transport and vertical motion from correlations between in situ measurements in the Airborne Antarctic Ozone Experiment, *J. Geophys. Res.*, *94*, 11,669–11,685, 1989.

Newman, P. A., D. J. Lamich, M. Gelman, M. R. Schoeberl, W. Baker, and A. Krueger, Meteorological atlas of the southern hemisphere lower stratosphere for August and September 1987, *NASA Tech. Memo.*, *4049*, 1988.

Podolske, J. R., M. Loewenstein, S. E. Strahan, and K. R. Chan, Stratospheric nitrous oxide in the southern hemisphere, *J. Geophys. Res.*, this issue.

Proffitt, M. H., J. A. Powell, A. F. Tuck, D. W. Fahey, K. K. Kelly, A. J. Krueger, M. R. Schoeberl, B. L. Gary, K. R. Chan, M. Loewenstein, and J. R. Podolske, A chemical definition of the boundary of the Antarctic ozone hole, *J. Geophys. Res.*, *94*, 11,437–11,448, 1989.

Proffitt, M. H., M. J. Steinkamp, J. A. Powell, R. J. McLaughlin, O. A. Mills, A. L. Schmeltekopf, T. L. Thompson, A. F. Tuck, T. Tyler, R. H. Winkler, and K. R. Chan, In situ ozone measurements within the 1987 Antarctic ozone hole from a high-altitude ER-2 aircraft, *J. Geophys. Res.*, this issue.

Schoeberl, M. R., et al., Reconstruction of the constituent distribution and trends in the Antarctic polar vortex from ER-2 flight observations, *J. Geophys. Res.*, this issue.

Swinbank, R., The global atmospheric angular momentum balance inferred from analyses made during the FGGE, *Q. J. R. Meteorol. Soc.*, *111*, 977–992, 1985.

Toon, G. C., C. B. Farmer, L. L. Lowes, P. W. Schaper, J.-F. Blavier, and R. H. Norton, Infrared aircraft measurements of stratospheric composition over Antarctica during September 1987, *J. Geophys. Res.*, this issue.

Tuck, A. F., Synoptic and chemical evolution of the Antarctic vortex in late winter and early spring 1987, *J. Geophys. Res.*, *94*, 11,687–11,737, 1989.

Tuck, A. F., R. T. Watson, E. P. Condon, J. J. Margitan, and O. B. Toon, The planning and execution of ER-2 and DC-8 aircraft flights over Antarctica, August and September 1987, *J. Geophys. Res.*, *94*, 11,181–11,222, 1989.

Watterson, I. G., and A. F. Tuck, A comparison of the longitudinal distributions of polar stratospheric clouds and temperatures for the 1987 Antarctic spring, *J. Geophys. Res.*, this issue.

K. R. Chan, M. Loewenstein, J. R. Podolske, and S. E. Strahan, NASA Ames Research Center, Moffett Field, CA 94035.

B. L. Gary, Jet Propulsion Laboratory, Pasadena, CA 91109.

K. K. Kelly, J. A. Powell, and M. H. Proffitt, NOAA Aeronomy Laboratory, 325 Broadway, Boulder, CO 80303.

(Received July 15, 1988;
revised April 14, 1989;
accepted April 14, 1989.)